Tellus (1990), *42A*, 28–40

The statistical properties of the interaction of high-frequency eddies with mountains in a two-layer model

By A. BUZZI, P. MALGUZZI and A. TREVISAN, *FISBAT-CNR, c/o Dipartimento di Fisica, Via Irnerio 46, I40126, Bologna, Italy*

(Manuscript received 7 December 1988; in final form 20 February 1989)

ABSTRACT

Long-term integrations of a two-layer quasi-geostrophic model are performed in the presence of idealized topography representing the Alps and the Rocky Mountains. The same techniques applied to observations are applied to the model results. On the one hand, the statistical properties of high-frequency eddies are compared with those deduced from observations. On the other hand, a comparison with the predictions of linear theory is made possible by the use of a linearized version of the same model. Modifications induced by orography in the nonlinear experiments compare well with those predicted by linear theory, including storm-track splitting and changes of eddy structure and symmetry near the two different topographic features.

1. Introduction

Travelling disturbances of the middle and high latitudes, that are generally identified as baroclinic waves (Blackmon et al., 1984a, b), are strongly influenced by the presence of mountains. In particular, important properties of transient eddies, such as propagation direction and speed, vertical and horizontal structure and growth rate, appear to be consistently different near mountains from those observed over flat surfaces (see, for example, Hess and Wagner, 1948; Murakami and Nakamura, 1983). A rather extensive statistical evidence of the effects that mountains exert on high-frequency (periods less than 6–8 days) atmospheric variability are presented in recent papers by Hsu (1987) and Buzzi and Tosi (1989; hereafter referred as BT).

Orographic cyclogenesis is one important and well-documented aspect of the influence of orography on baroclinic waves (Petterssen, 1956; Newton, 1956; Palmén and Newton, 1969; Smith, 1979). BT discuss how lee cyclogenesis leaves a signature in some statistical indicators of geopotential fields near mountains and how lee cyclogenesis can be viewed in terms of the more general class of phenomenology regarding the high-frequency variability of the atmosphere in the proximity of mountains. In particular, by analysing areas comprising the Alps and the Rocky mountains, BT show that the high-pass filtered low-level standard deviations fields, cross-correlation fields between lower and upper levels and one-point correlation maps show statistically significant alterations near those mountains ranges. These alterations possess horizontal scales typical of the eddies themselves, that is about 1000 km (corresponding to zonal wavelengths of 3000–4000 km). The mountain-induced features are consistent, in both areas, with those exhibited by lee cyclogenesis events (where the word "lee" refers to the southern side of the Alps and to the eastern side of the Rockies). However, BT show that these features are not exclusively due to the cumulative effects of lee cyclogenesis, being typical of moving eddies of different intensity and characterizing both negative and positive (cyclonic and anticyclonic) anomalies.

BT also compare their statistical results, based on ECMWF data analyses, with those predicted by different available theories of cyclogenesis in the lee of the Alps and the Rocky Mountains, and of propagation of disturbances in the vicinity of large-scale mountains. The modifications induced by topography on the normal modes of baroclinic instability, invoked to explain the basic mechanisms of orographic cyclogenesis (hereafter referred to as the normal mode theory of lee cyclogenesis: Speranza et al., 1985; Buzzi and Speranza, 1986; Malguzzi et al., 1987; Buzzi et al., 1987; Trevisan et al., 1988), appear to be consistent with many of the observed statistics of the high-pass disturbances in the areas of mountains (BT).

However, this theory was formulated in terms of linear normal modes of a baroclinically unstable zonal flow. A direct comparison of observed atmospheric variability with the properties of linear normal modes is not straightforward. The most serious problem is related to the difficulties encountered in defining a "basic state" around which to linearize the equations (see, for instance, Pedlosky, 1986) and to the fact that nonlinear effects, related to both "wave–wave" and "zonal flow–wave" interactions, may dominate the properties of the turbulent state of the real atmosphere.

At the present stage of our knowledge, a complete solution of the problem mentioned above would be an almost impossible task. The purpose of this paper is to provide a self-consistent check between linear normal mode analysis of unstable disturbances influenced by orography and the effect of orography on the statistics when the system is in a chaotic regime. To perform this task, we compare, on the one hand, statistical properties of long time series of real data with analogous statistical properties of long-term numerical runs. On the other hand, we compare the model runs, in which model realizations can be considered to belong to the model attractor (for a particular choice of the external parameters) with linear properties computed for the same model. We have used a two-layer, quasi-geostrophic model, that is simple enough to gain a physical understanding of its main properties and to allow affordable long-term runs in order to define its own "climate" (many years of integration are needed to obtain good statistical confidence).

The numerical experiments, performed under different controlled conditions, have been diagnosed using the same techniques applied by BT to the atmospheric observations. We show that the modelled eddy structure, as well as other statistical properties of the high-frequency variability, are similar, near the orography, to that observed in real data. Moreover, we show that these properties compare well with those derived from normal modes computed with the same model. We then discuss the physical consequences and deductions that can be inferred from such a comparison.

2. The model

The interpretation of lee cyclogenesis in terms of the normal mode theory involves several approximations which are difficult to evaluate in real data. A numerical model allows both computation of normal modes (around some basic state to be suitably defined) and statistical analysis through long-term time integrations. On the one hand, it is feasible to compare statistical analysis performed on real data with similar analyses performed on the corresponding model quantities. On the other hand, the interpretation of the statistical properties of the model evolution in terms of normal mode theory performed on the same model is certainly more straightforward (although not an easy task to do) than for the atmosphere itself.

The numerical model chosen to perform the above-mentioned task is a two-layer, quasi-geostrophic model in a β-plane, periodic channel, 10,000 km wide, and 20,000 km long. The flow is forced by a relaxation (time constant of 10 days) towards a radiative–convective symmetric equilibrium. Dissipation is included through an Ekman layer at the lower boundary (dissipative time constant of 4 days) and momentum exchange between the upper and lower layer (time constant of 10 days). The mathematical formulation of the model can be found in Lorenz (1963). The lower boundary condition, applied at $z = 0$, states that the vertical velocity is given by $w = uh_x + vh_y$, where the topography $h(x, y)$ is chosen to schematically reproduce the shape of the Alps and the Rocky Mountains. For the case of the Alps:

$$h = h_0 \exp(-x^2/x_0^2) \exp(-y^2/y_0^2),$$

$$h_0 = 3 \text{ km}, \quad x_0 = 900 \text{ km}, \quad y_0 = 350 \text{ km}.$$

Such a mountain, centred in the middle of the domain, is chosen in order to reproduce the symmetry invoked by the normal mode theory of Alpine cyclogenesis, i.e., an east–west elongated mountain parallel to the mean zonal wind (Speranza et al., 1985). The mountain volume is large enough to allow a qualitatively correct response in the limits of the quasi-geostrophic approximation (Malguzzi et al., 1987).

For the case of the Rocky Mountains:

$h = h_0 \exp(-x^2/x_0^2)\, f(y),$

$f(y) = \frac{1}{2}\{1 - \tanh[(y - y_0)/s]\}, \quad y \geqslant 0,$

and $f(-y) = f(y),$

$h_0 = 3$ km, $x_0 = 500$ km, $y_0 = 2500$ km,

$s = 1000$ km.

This particular meridional profile is more suitable for representation of a north–south oriented ridge like the Rockies. These two choices of topographic shapes, besides being a schematic description of real cases, represent the two limiting cases of topographic ridges parallel and perpendicular to the basic flow, respectively.

The horizontal resolution necessary to appropriately describe the effects of the topography is different in the two cases. For the case of the Alps (Rockies), the model variables are discretized on a latitudinal grid of about 150 (230) km mesh size, while the longitudinal dependence is represented by 12 (16) Fourier modes. An Euler scheme is used for the time integration; horizontal diffusion of the smallest scales is included to prevent numerical errors.

An important parameter is the equator-to-pole temperature difference of the radiative equilibrium which controls the degree of chaos present in the model evolution. Such temperature contrast has been set equal to 40°K, a value which gives a reasonable zonal jet in the upper layer and chaotic evolution of the model variables. In particular, it turns out (see Section 3) that the model variance pertaining to the high-frequency part of the spectrum is comparable to the same quantity computed from real data.

The length of the channel is a compromise between computational costs and the need to include long-wave components. In fact, if the dynamics of the wavelengths of interest (i.e., the most unstable baroclinic waves) has to be properly described, longer waves must be included in order to allow for nonlinear energy cascade. Fig. 1 shows the wavenumber–frequency power spectrum obtained in a reference experiment with a flat bottom, which consists in the integration of the model for 6 years, keeping the thermal forcing constant. A high-frequency peak of wave activity, characterized by periods in the range from 5 to 7 days, appears at model wavenumber 5, which is typical of baroclinic instability. Wavenumber 4 is also baroclinically unstable, and indeed there exists a maximum in the spectrum at this wavelength with periods

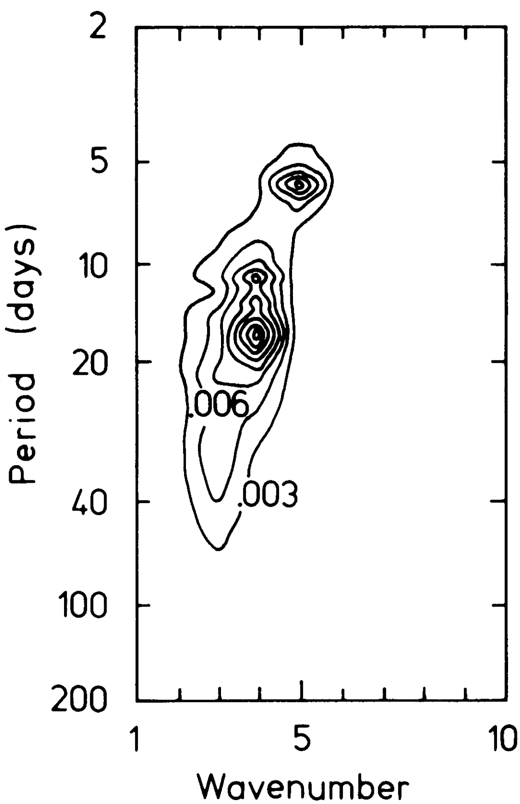

Fig. 1. Space-time power spectrum (normalized by period T) of the cosine coefficient of the barotropic part of the streamfunction, computed in the centre of the channel. The zonal wavenumbers (abscissa) are referred to the channel length (20,000 km in dimensional units). The ordinate scale (period T) is logarithmic. Contour interval is 0.003 in adimensional units, corresponding to 30 m^2 in dimensional units.

between 10 and 20 days. However, in this work, we focus on the statistical properties of high-frequency eddies which present an isolated maximum in the spectrum, and which have already been studied in real data.

For either topography, one experiment lasting 6 years of perpetual (intermediate) season has been performed. This duration is required for statistical significance. The initial 40 days of integration have not been included in the diagnostics, since roughly, this interval is spent by the system to reach its attractor.

3. Experiment results and comparison with real data

3.1. *Alps*

In this section, we describe some statistical quantities computed from the 6 years experiment in the presence of topography simulating the Alps. Some of these quantities have been derived from a high-pass filtered streamfunction in the upper and lower layer. The filter used (see BT for more details) has a steep cut-off around 8 days: this choice is suggested by inspection of the spectrum (Fig. 1); no appreciable changes are introduced in the spectrum by the topography.

Fig. 2 shows the streamfunction time mean and the high-pass standard deviation, in the upper and lower layer, respectively. The time mean shows little influence of the orography on the upper level flow, while the orographically induced anticyclonic anomaly is the main feature of the lower layer climatology. This particular feature is not observed in real data (see Fig. 2 of BT) for several reasons. Among these are the mountain shape, the presence of large-scale waves, the non-zonality and northward displacement of the storm-track with respect to the real Alps. Clearly, the large-scale disturbances are strongly influenced by the lack of realism in the non-symmetric forcing (planetary scale mountains, land–sea contrast, etc.). As far as the standard deviation is concerned, we observe that the magnitude of geopotential fluctuations in this

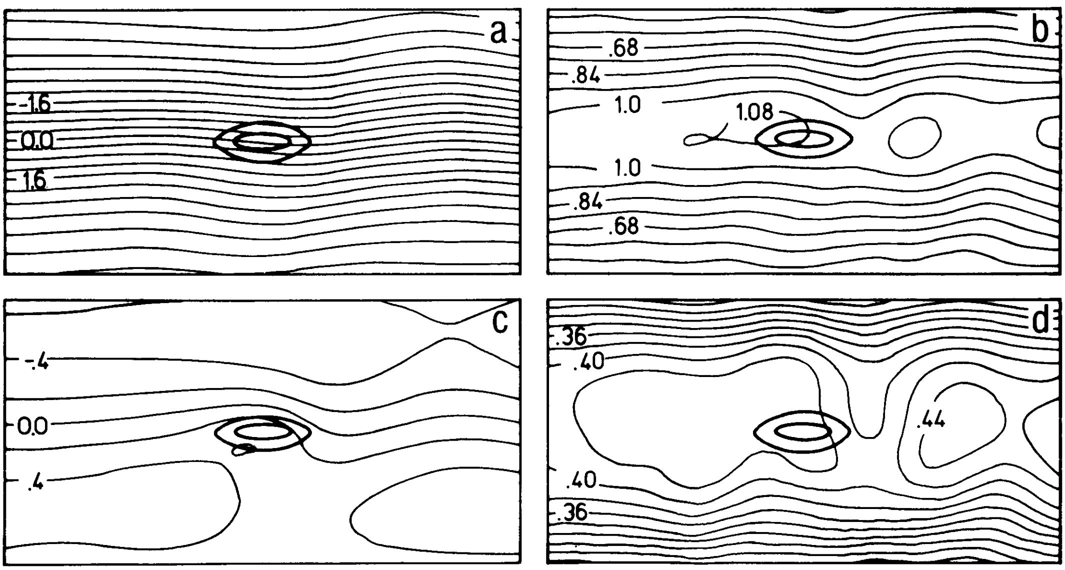

Fig. 2. Experiment with idealized Alps. The area represented is a "window" 10,000 km long (half of the total domain length) and 5,000 km wide (half of the channel width). Mountain contours represent the 1 km and 2 km height, respectively. (a) Time mean of the streamfunction in the upper layer. Contour interval: 0.4 (adimensional units). (b) Standard deviation of the high-pass filtered (periods less than 8 days) fluctuations of the streamfunction in the upper layer. Contour interval: 0.08. (c) As (a), but in the lower layer and with contour interval: 0.2. (d) As (b), but in the lower layer and with contour interval: 0.02.

model is comparable to that deduced from observations (see Fig. 2 of BT). The most significant feature appears in Fig. 2d, which shows the topographic effect on the strength of high-frequency eddies. The storm-track tends to be interrupted to the north of the mountain and to deviate to the south, while, downstream, it returns to its undisturbed position in the centre of the channel. Although, for the reasons discussed above, there is no close similarity between the 850 hPa variance and the lower layer model variance, the effect of the mountain is in agreement with observations that variability is enhanced south of the orography and hindered on its northeastern side.

Even more striking is the similarity with observations of another statistical feature that we consider as a typical signature of lee cyclogenesis: the cross-correlation between high-frequency geopotential fluctuations at lower and upper levels (Fig. 3b). In the real data (Fig. 3a), the "dipolar" distribution of correlation across the Alps and the other mountain ranges of Southern Europe and Turkey is most evident. The strong correlation gradient across the topography contrasts with the almost uniform distribution over the Atlantic. Fig. 3a documents the spatial scale of the correlation distribution and its close relation with the underlying topography. The similarity between Figs. 3a, b is evident, in spite of the very simple geometrical shape of the model topography. This suggests that the Alps and the surrounding mountain chains can be reduced to a mountain having a symmetry hypothesized in the normal mode theory of lee cyclogenesis, i.e., a ridge oriented along the baroclinic basic flow.

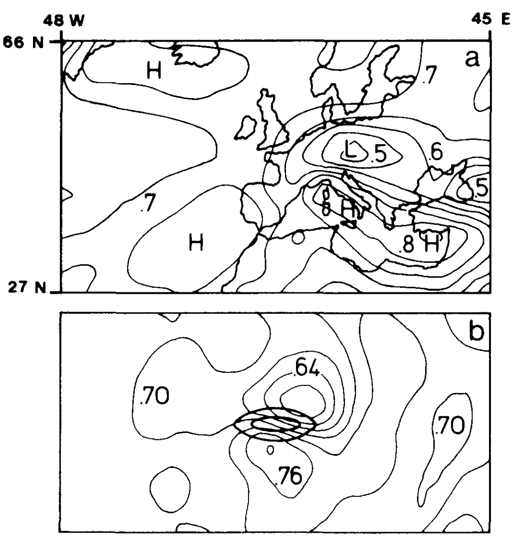

Fig. 3. (a) Cross-correlation between high-pass filtered 850 hPa height and high-pass filtered 500 hPa height, derived from ECMWF analyses (Buzzi and Tosi, 1989). (b) As (a), but between the upper and the lower layer high-pass filtered streamfunction, in the experiment with idealized Alps. Contour interval: 0.03. At 99% confidence limit, the confidence interval is about 0.08 for (a) and 0.05 for (b).

We interpret the cross-correlation distribution as being due to the different mean phase-shift between upper and lower level pressure fluctuations; this implies that waves are more "baroclinic" north than south of the mountain. These differences in the vertical phase-shift can in turn be identified as being due to the mountain-induced dipolar perturbation on baroclinic waves, which has been observed in numerical experiments based on individual cases of lee cyclogenesis and is predicted by normal mode theory (Speranza et al., 1985).

Fig. 3 is an example of a statistical indicator that reveals the modification due to orography of the spatial structure of high-frequency disturbances, particularly as far as the vertical organization is concerned.

We consider now the modifications of the horizontal structure of the eddies. The one-point lagged covariance (or correlation) maps are a simple but efficient tool to provide insight into the horizontal structure (see, for example, Hsu, 1987; Wallace et al., 1988; BT). Fig. 4 shows one-point lagged covariances of the lower layer, high-pass filtered geopotential height, computed for the case of the idealized Alps and for different lag times. We show covariances rather than correlations, because covariances can be closely compared with the structure of the eigenmodes (see Section 5). However, the correlation fields, being weighted with the standard deviation (see Fig. 2d), simply give less meridionally confined structures than covariances. The base point is chosen upstream of the topography and in the middle of the channel; different choices of the base point along the storm-track do not appreciably affect the spatial structure of the correlation fields. Fig. 4f contains the "storm track"

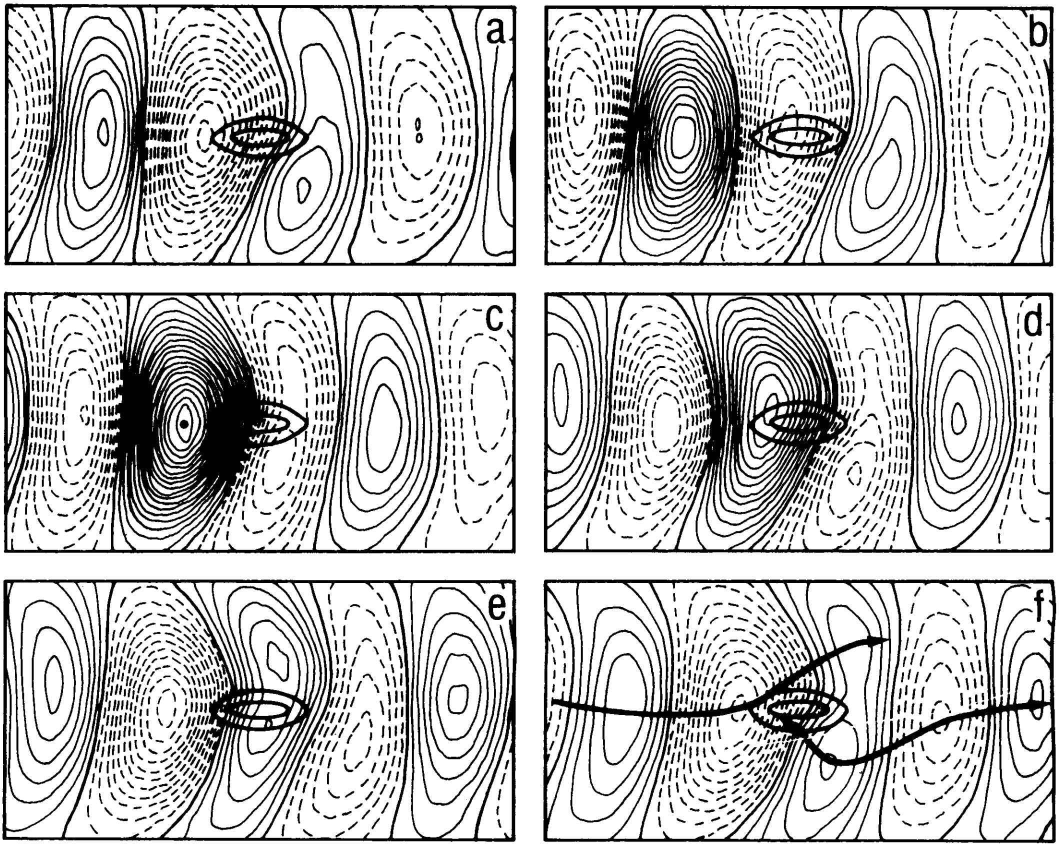

Fig. 4. Maps of lagged covariances between high-pass filtered streamfunction at the base point marked by a dot in (c) and high-pass filtered streamfunction at all other points, in the lower layer, for the experiment with idealized Alps. (a), (b), (c), (d), (e) and (f) correspond to lag times of −2, −1, 0, 1, 2, 3 days, respectively. Contour interval: 0.01. In (f) the "storm track" is sketched.

obtained by joining the position of consecutive maxima or minima. We notice that the eddies approaching the mountain from the west undergo a decay to the north of the mountain while a new maximum appears to the south of it. This new maximum amplifies and then moves downstream, finally recovering the original position in the centre of the domain. The entire process cannot be described simply as a splitting around the mountain of the incoming eddy: in fact, we observe decay and acceleration to the north and growth and deceleration to the south. Therefore, the phase lines also become distorted near the mountain.

Fig. 4, (a) through (f), spanning a total of 5 days of lag intervals, describes almost one entire cycle (one period) of the eddy field (see also Fig. 1). One should note the rather high coherence in time and space of the eddies, once the low-frequency components are removed. Statistically significant correlation values are found at more than one wavelength distance from the base point and for lag times of the order of a few days (for an evaluation of the statistical confidence, see BT; note also that the model coherence is higher than for real data).

A comparison between Fig. 4 and Fig. 6 of BT indicates that there is very good agreement between the behaviour of the eddies passing near the real Alps and those described in our model.

The only region where real data and model results are not very similar is downstream of the mountain. However, we recall that in nature, the orographic action of the Alps is prolonged downstream by the presence of an almost uninterrupted mountain range reaching the Anatolian peninsula.

The 4000 km mean wavelength observed in Fig. 4 compares well with the wavelength typical of observed baroclinic disturbances. The phase speed, however, is slower in the model than in reality, also reflecting the larger typical periods (about 5.5 days against about 3.5 days), but this is a well-known deficiency of the two-layer model.

Fig. 4 provides information on the eddy structure without discriminating between the signs of the anomalies (positive: anticyclonic; negative: cyclonic). This discrimination can be obtained by computing the lagged composite maps (see, for instance, BT). These maps are not shown here for the reason that they indicate very similar, statistically indistinguishable behaviours of the positive and negative high-frequency anomalies. The most coherent signal is obtained for relatively high amplitude eddies (for instance, larger than one standard deviation in the centre of the storm-track). This property is found by BT to also hold in real data. It indicates that the modification induced by the orography on the travelling disturbances is similar, but with opposite sign, for cyclones and anticyclones.

3.2. *Rocky Mountains*

The experiment climatology for the Rocky Mountain case is shown in Fig. 5. The mountain modifies, on average, the flow in a more appreciable way than the idealized Alps. In the lower

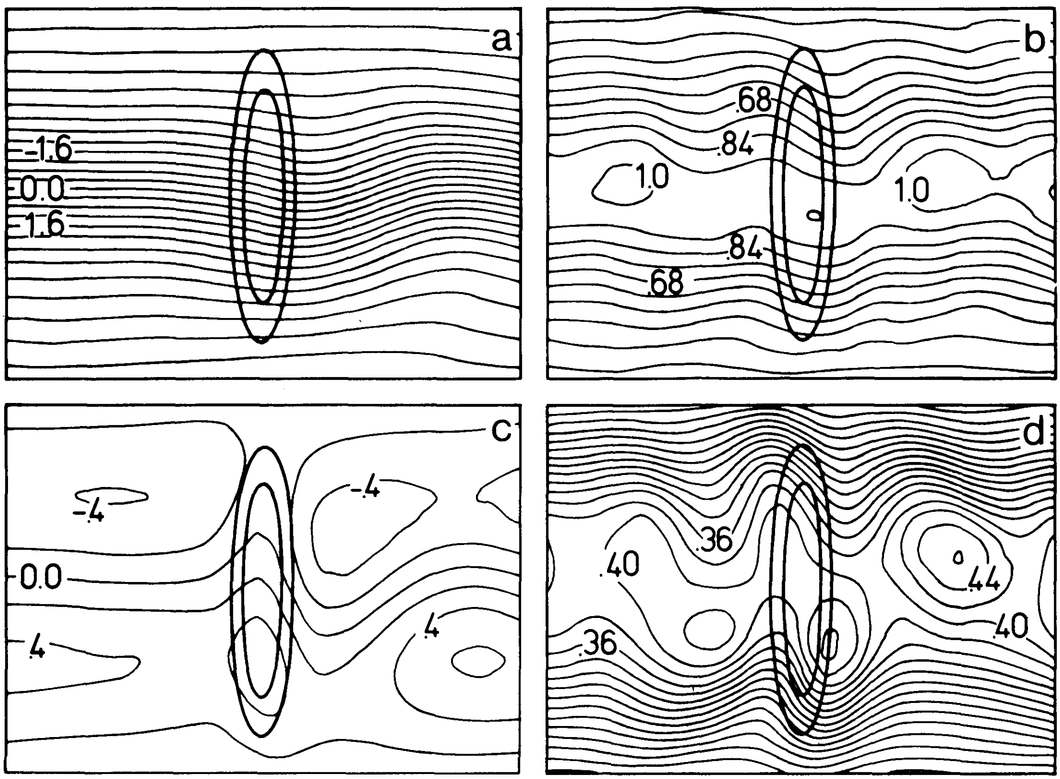

Fig. 5. As Fig. 2, but for the experiment with the idealized Rockies. The display window is extended to a width of 7273 km.

layer (Fig. 5c), we observe, on average, a ridge over the mountain and a pronounced trough downstream of it. These features are observed in the real case (see Fig. 12 of BT). In the upper layer, the ridge is absent (in contrast with observations) and the trough is displaced somewhat westward.

In the lower layer, the high-pass filtered standard deviation presents features that compare well with observations: in particular, the isolated maximum in the lee is identifiable with the "Colorado" maximum. Other common features are the two minima of high-frequency variability located south-west and north-east of the moun-

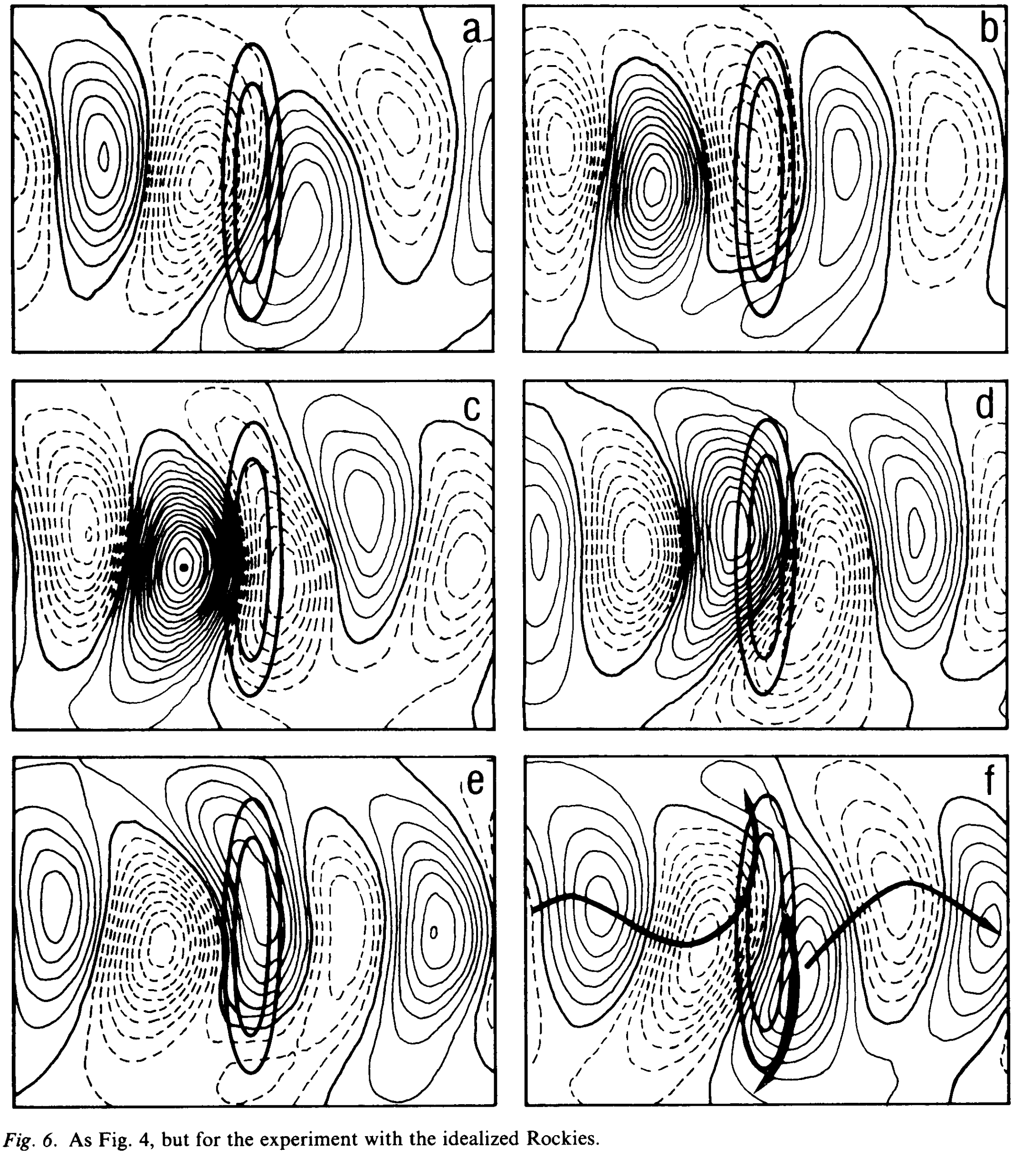

Fig. 6. As Fig. 4, but for the experiment with the idealized Rockies.

tain. The storm track (see also below) recovers its original position far downstream of the mountain; the maximum observed downstream in Fig. 5d is due to eddy modifications which may be caused either by direct interaction with the mountain or by the interaction with the modified, slowly varying part of the flow. However, linear analysis (see Section 4) indicates that eddy modifications in the vicinity of the mountain may be accounted for only in terms of direct interaction with the mountain itself.

We point out that since we focus only on the eddy structure, the high-pass filtered fields shown here do not include the zonally averaged component of geopotential. This component contains high-frequency oscillations due to the form drag exerted by the mountain in response to the passage of high-frequency eddies. This effect is over-represented in our model, due essentially to the large ratio between the mountain volume and total domain volume.

Fig. 6, (a) through (f), shows one-point lagged covariances for the Rocky Mountains case. The "storm track" is shown in Fig. 6f. We observe that the trajectory of the eddies is highly distorted by the ridge. We notice that the incoming eddies are deviated to the north by the mountain and that a new maximum suddenly appears in the downstream lee. This maximum seems to "split" again (see Figs. 6d, e); one of the new maxima moves southward along the mountain contours and decays, while the other moves eastward with the mean flow. Fig. 7 shows the eddy storm track in the real case in winter, using the same data set analysed in BT (see also Hsu, 1987). A close similarity is observed in the behaviour near the mountain, incuding the northward deviation, the sudden appearance of a new track and its subsequent splitting.

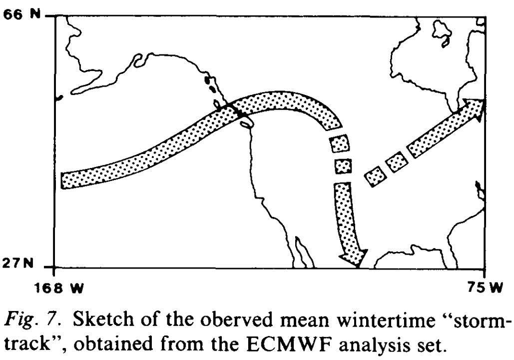

Fig. 7. Sketch of the oberved mean wintertime "storm-track", obtained from the ECMWF analysis set.

4. Comparison with linear theory

The difficulties presented by any attempt to compare a linear theory of baroclinic instability with nonlinear dynamics are well-known (Gall, 1976; Pedlosky, 1986; Speranza and Malguzzi, 1988). Apart from this unavoidable difficulty, the only reasonable procedure consists in comparing nonlinear evolutions and linear theory within the framework of a same model approximation, provided this model contains the essential physical processes that characterize the atmospheric time evolution we are interested in.

In this section, we compare the statistical properties described in Section 3 with linear theory performed on the same model. In doing this, we will focus on the modifications, introduced by orography, both on the nonlinear evolution and on linear normal modes.

Figs. 8 through 10 show some properties of the most unstable normal mode for the case of the idealized Alps. This mode has been obtained by

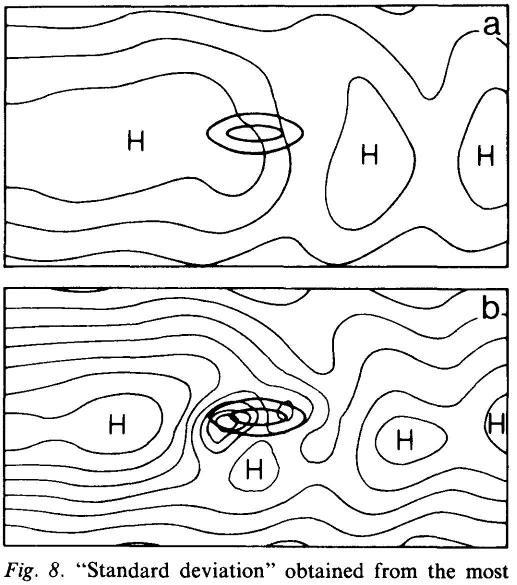

Fig. 8. "Standard deviation" obtained from the most unstable mode, in the case of idealized Alps, assuming random phases and no growth in time. (a) Upper layer. (b) Lower layer. The contour interval in (b) is one half of the contour interval in (a).

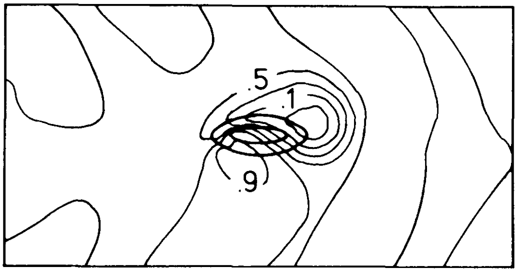

Fig. 9. Cross-correlation between the upper and the lower layer, obtained from the most unstable normal mode, computed in the case of idealized Alps, assuming random phases and no growth in time. Contour interval: 0.2.

integrating (for a sufficiently long time) the linearized version of our model, starting from an arbitrary initial condition. The modes have been normalized throughout in such a way that the maximum in the meridional structure of the dominant zonal wavenumber is unity. Among the possible choices of an unstable basic state, we have selected the model Hadley circulation (Pedlosky, 1986), which has zero wind in the lower layer.

It can be readily seen from comparison with Figs. 2, 3 and 4, that several features of topographic modifications are well captured: in particular, the maximum of the standard devi-

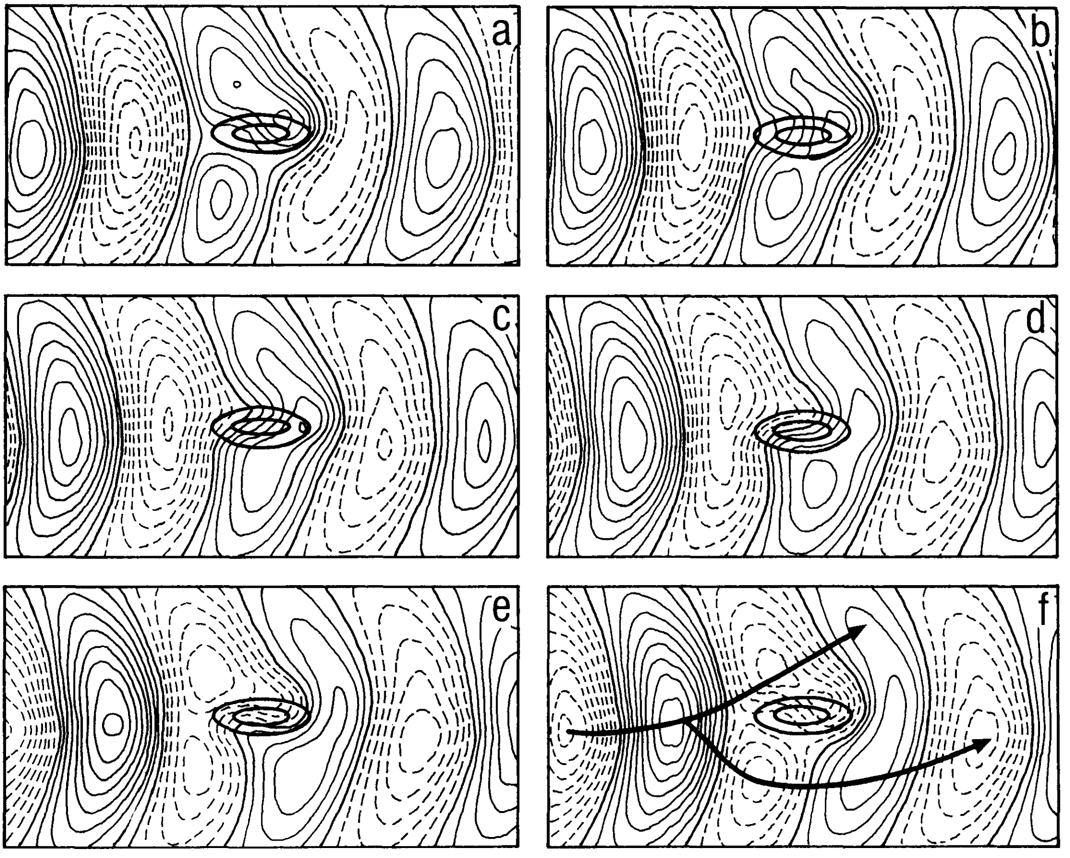

Fig. 10. Streamfunction of the most unstable normal mode, computed in the case of idealized Alps in the lower layer at different phases, corresponding to time intervals of 1 day, and normalized to the same total amplitude. The amplitude is arbitrary.

ation in the lee of the mountain and the minimum downstream (Figs. 2d, 8b); the dipolar feature in the upper-to-lower layer geopotential correlation (Figs. 3b, 9); and the storm track splitting (Figs. 4, 10). However, there are also some differences in the field of topographic modifications: in particular, the minimum (maximum) at the western (eastern) corner of the mountain in the standard deviation field (Fig. 8b) are overpredicted by linear theory. Inspection of Fig. 10 shows that these features are associated with a premature splitting of the storm track, with an isolated maximum (minimum) of geopotential height moving eastward along the northern side of the mountain contours.

In comparing the linear with the nonlinear results, one should keep in mind that while the linear results are "deterministic", the nonlinear results are evaluated with statistical indicators which average over different episodes and chaotic fluctuations. This may explain the apparent "oversensitivity" of the normal modes to orographic modifications. An inspection of the numerical fields indicates that some individual cyclogenetic events in the lee of model mountains have characteristics very similar to modal structure, although the purpose of this paper is not that of diagnosing single cases which may not be representative of a mean behaviour.

Figs. 11 and 12 show, respectively, the standard deviation and a 6-day sequence of the most unstable normal mode computed for the case of the idealized Rocky Mountains. The field of standard deviation in the lower layer computed for the normal mode is in close qualitative agreement with that computed from the experiment (Figs. 5d, 11b), particularly in the region near the mountain; note that Fig. 11b contains the "Colorado maximum" and the tongues of low standard deviation on the north-west and south-east sides of the mountain.

Strikingly similar are the topographically induced modifications of the storm track (Figs. 6f, 12f). Linear theory predicts well the storm track split into the 3 branches, commented upon in Subsection 3.2. As far as the southward moving branch of Fig. 12f is concerned, topographic Rossby wave propagation has been suggested as a relevant dynamical balance (Newton, 1956; Hsu, 1987). How this interpretation can be incorporated in the present theory is discussed in BT.

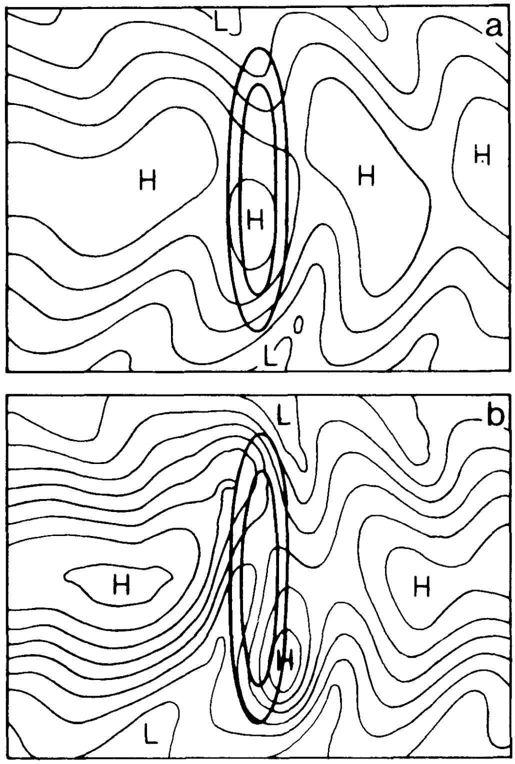

Fig. 11. As Fig. 8, but for the case of the idealized Rockies.

5. Conclusions

The important effect of orography in determining eddy propagation and structure, as revealed by statistical analyses of high-frequency eddies in the vicinity of mountains (BT), has been studied in a simple, two-layer quasi-geostrophic model.

Long-term integrations have been performed in a periodic channel, with constant forcing and different orographies, representing idealizations of the Alps and the Rockies, respectively. The simulated statistics, notwithstanding the model simplicity, exhibit many features in common with those obtained from observations, particularly as far as the orographically induced perturbation on eddy structure and propagation are concerned.

A direct comparison of the model statistics with the structures obtained from normal mode

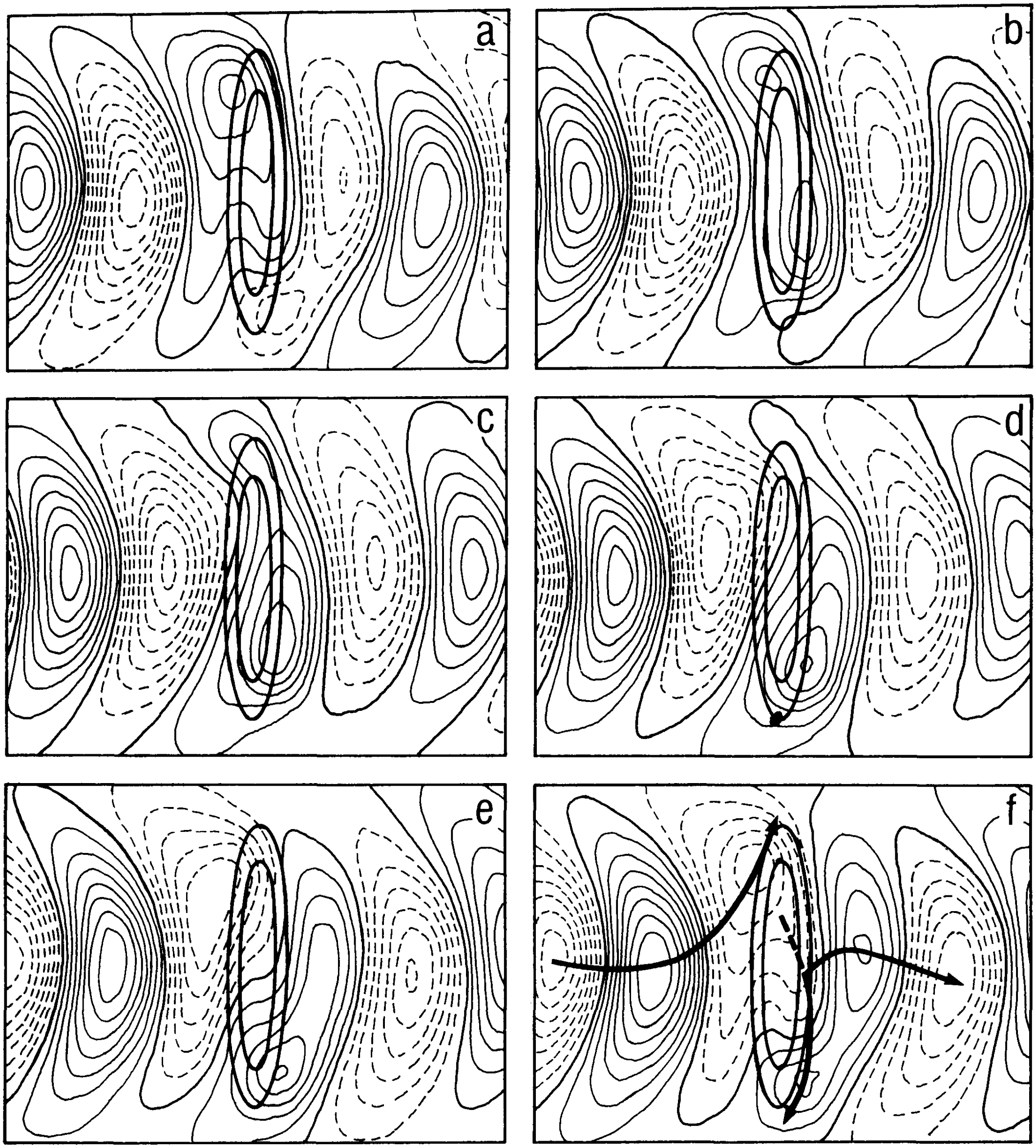

Fig. 12. As Fig. 10, but for the case of the idealized Rockies.

analysis of baroclinic waves in the presence of topography is now feasible and sheds light on the significance and limits of linear theory. Such a theory has been shown to be capable of reproducing some of the observed features characterizing fully developed travelling eddies modified by orography. We note that the application of time filtering together with the statistical approach allow for a better comparison between theory and fully nonlinear model behaviour.

The tentative conclusions derived by direct comparison with atmospheric statistics (BT) have been confirmed by the results of the model experiments. We have shown that the modifications induced by the orography on the high-frequency eddies in the nonlinear experiments and the modifications induced by the orography on the normal modes are very similar to each other, indicating that normal mode theory reproduces the basic physical ingredients of the interaction between travelling baroclinic waves and mountains.

REFERENCES

Blackmon, M. L., Lee, Y.-H. and Wallace, J. M. 1984a. Horizontal structure of 500 mb height fluctuations with long, intermediate and short time scales. *J. Atmos. Sci. 41*, 961–979.

Blackmon, M. L., Lee, Y.-H., Wallace, J. M. and Hsu, H.-H. 1984b. Time variations of 500 mb height fluctuations with long, intermediate and short time-scales as deduced from lag-correlation statistics. *J. Atmos. Sci. 41*, 981–991.

Buzzi, A. and Speranza, A. 1986. A theory of deep cyclogenesis in the lee of the Alps. Part II: Effects of finite topographic slope and height. *J. Atmos. Sci. 43*, 2826–2837.

Buzzi, A., Speranza, A., Tibaldi, S. and Tosi, E. 1987. A unified theory of orographic influences upon cyclogenesis. *Meteorol. Atmos. Phys. 36*, 91–107.

Buzzi, A. and Tosi, E. 1989. Statistical behaviour of transient eddies near mountains and implications for theories of lee cyclogenesis. *J. Atmos. Sci. 46*, May 1989.

Gall, R. 1976. A comparison of linear baroclinic instability theory with eddy statistics of a general circulation model. *J. Atmos. Sci. 33*, 349–373.

Hess, S. L. and Wagner, H. 1948. Atmospheric waves in the northwestern United States. *J. Meteor. 5*, 1–19.

Hsu, H.-H. 1987. Propagation of low-level circulation features in the vicinity of mountain ranges. *Mon. Wea. Rev. 115*, 1864–1892.

Lorenz, E. N. 1963. The mechanics of vacillation. *J. Atmos. Sci. 20*, 448–464.

Malguzzi, P., Trevisan, A. and Speranza, A. 1987. Effects of finite height topography on nongeostrophic baroclinic instability: implications to theories of lee cyclogenesis. *J. Atmos. Sci. 44*, 1475–1482.

Murakami, T. and Nakamura, H. 1983. Orographic effects on cold surges and lee-cyclogenesis as revealed by a numerical experiment. Part I: Transient aspects. *J. Meteor. Soc. Japan 61*, 547–567.

Newton, C. W. 1956. Mechanisms of circulation change during a lee cyclogenesis. *J. Meteor. 13*, 528–539.

Palmén, E. and Newton, C. W. 1969. *Atmospheric circulation systems*. New York: Academic Press, 603 pp.

Pedlosky, J. 1986. *Geophysical fluid dynamics* (Second ed.). New York: Springer-Verlag, 710 pp.

Petterssen, S. 1956. *Weather analysis and forecasting*. Vol. I. New York: McGraw-Hill Book Co., 428 pp.

Smith, R. B. 1979. The influence of mountains on the atmosphere. *Advances in geophysics, 21*. New York: Academic Press, 87–230.

Speranza, A., Buzzi, A., Trevisan, A. and Malguzzi, P. 1985. A theory of deep cyclogenesis in the lee of the Alps: modifications of baroclinic instability by localized topography. Part I. *J. Atmos. Sci. 42*, 1521–1535.

Speranza, A. and Malguzzi, P. 1988. The statistical properties of a zonal jet in a baroclinic atmosphere: a semilinear approach. Part I: Quasigeostrophic, two-layer model atmosphere. *J. Atmos. Sci. 45*, 3046–3061.

Trevisan, A., Ferranti, L. and Malguzzi, P. 1988. Further developments of normal mode theory of lee cyclogenesis: isentropic coordinate model. *J. Atmos. Sci. 45*, 3880–3888.

Wallace, J. M., Lim, G. H. and Blackmon, M. L. 1988. Relationship between cyclone tracks, anticyclone tracks and baroclinic waveguides. *J. Atmos. Sci. 45*, 439–462.